

## Sandpile model with activity inhibition

S. S. Manna\* and D. Giri†

*Department of Physics, Indian Institute of Technology, Powai, Mumbai 400 076, India*

(Received 25 June 1997)

A sandpile model is studied in which bonds of the system are inhibited for activity after a certain number of transmission of grains. This condition impels an unstable sand column to distribute grains only to those neighbors that have toppled less than  $m$  times. In this non-Abelian model grains effectively move faster than the ordinary diffusion (superdiffusion). A system size dependent crossover from Abelian sandpile behavior to a new critical behavior is observed for all values of the parameter  $m$ . [S1063-651X(97)51111-1]

PACS number(s): 05.40.+j, 05.70.Jk, 05.70.Ln

The concept of self-organized criticality (SOC) was introduced to describe how a system, starting from an arbitrary initial condition may evolve to a scale free critical state following some specific dynamical rules while under the action of repeated external perturbations [1]. Naturally occurring physical phenomena like sandpiles [2], forest fires [3], river networks [4], earthquakes [5], etc. are argued as systems showing SOC. To demonstrate the idea of SOC a simple model known as the ‘‘sandpile’’ model was introduced in which a stochastically driven cellular automata evolves under a nonlinear, diffusive, self-organizing mechanism leading to a nonequilibrium critical state [1].

At present many different versions of the sandpile model are available. However, precise classification of various models in different universality classes in terms of their critical exponents is not yet fully complete and still attracts much attention [6]. Among the different models most widely studied is the Abelian sandpile model (ASM) in which many analytical [7] as well as numerical [8] results are known. Some efforts have also been given towards the analytical calculation of avalanche size exponents [9,10]. Second, a two-state sandpile model with stochastic evolution rules was also studied [11] that was initially thought to belong to the same universality class as that of ASM [11,12] but later claimed to be different [13].

We consider a situation in which an intermediate time scale is associated with every bond of the system. Each bond allows only a certain number of grains to cross from its one end to the other and after that it has a dead time and cannot support any further traffic until a new avalanche starts. This dead time is much greater than the time scale of avalanche propagations but much less than the input rate of grains. We call this model as the ‘‘sandpile model with activity inhibition’’ (SMAI).

Similar to different sandpile models we also define our model on a regular lattice with open boundary. Non-negative integer numbers ( $h_i$ ) assigned at the lattice sites represent the heights of the sand columns. Sand grains are added at randomly chosen sites by increasing the  $h$  values by unity:  $h_i \rightarrow h_i + 1$ . The possibility of a sand column becoming unstable arises only when the height  $h_i$  becomes greater than a

threshold value  $h_c$ . Such a column becomes unstable only if the number  $n_i$  of nearest-neighbor sites that have toppled less than a preassigned cutoff number  $m$  within the same avalanche is found to be nonzero. An unstable column immediately topples and distributes one grain each to all the  $n_i$  neighbors:  $h_j \rightarrow h_j + 1$  ( $j = 1$  to  $n_i$ ). The sand column decreases by the same amount:  $h_i \rightarrow h_i - n_i$ . If  $n_i = 0$ , the sand column does not topple and its height, though greater than  $h_c$ , is considered stable. In an avalanche sites can topple a maximum of  $m$  times. This implies that in the limit of  $m \rightarrow \infty$  our model converges to ASM. Recently a stochastic sandpile model has been studied in which sand columns having heights greater than the threshold are also considered stable [14].

One unit of time within an avalanche consists of the following intermediate steps: (i) a list of all sites where  $h_i > h_c$  is made, (ii)  $n_i$  values are calculated for each site  $i$ , (iii) all sites with nonzero  $n_i$  values are toppled in parallel.

We first consider the case where the cutoff in the toppling number  $m = 1$ . Here the toppling front moves outwards and grains always jump only in the outward direction and do not fall back. Therefore, compared to the random walk analogy for the movement of the grains in ASM [15] in our model grains move faster than diffusing particles. This is indeed reflected in the average cluster size  $\langle s \rangle \sim L^{\beta_s}$ , where  $\beta_s = 1.62$  (reported below). This implies that the displacements  $\mathcal{R}$  of the grains in our model grows with time  $\mathcal{T}$  as  $\mathcal{R} \sim \mathcal{T}^\nu$  with  $\nu = 1/1.62 = 0.62$ , which is faster than diffusion (superdiffusion).

Zhang had studied a scaling theory of the sandpile model in which the toppling front grows as a  $(d-1)$  dimensional surface in the  $d$  dimension and multiple topplings were ignored [16]. Since, in SMAI, a single toppling front moves outward and multiple topplings are forbidden for  $m = 1$ , we expect that SMAI may be a correct realization of Zhang’s theory [16].

Unlike ASM our model turns out to be non-Abelian. Different steady state configurations are obtained on dropping grains at the same locations but following different sequences. On a stable configuration in a  $2 \times 2$  cell two grains are dropped at two sites using different sequences. Different final states are obtained (Fig. 1). Non-abelianity is effective only when avalanche cluster sizes are larger than 1.

A forbidden subconfiguration (FSC) in ASM is defined as the subset of connected sites for which at each site the height

\*Electronic address: manna@niharika.phy.iitb.ernet.in

†Electronic address: giri@niharika.phy.iitb.ernet.in

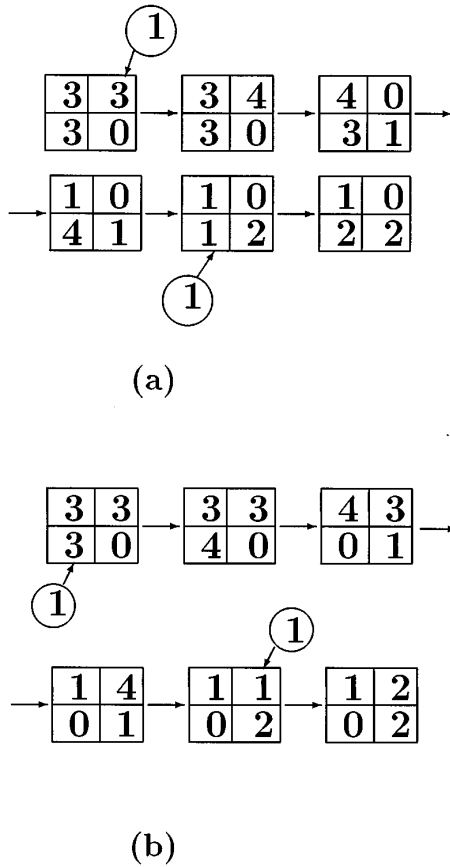


FIG. 1. Non-Abelian property of the sandpile model is shown on a  $2 \times 2$  cell. On the same initial stable configuration two grains are added at two different sites but in different orders. Different final stable configurations are obtained.

is less than its coordination number in the subset [7]. In SMAI also two neighboring sites whose heights are both zero (0—0) will never occur in the steady state because of the same reason as in ASM that if one topples the other site will receive one grain. Similarly a height configuration like (0—1—0) is also an FSC. In fact, all the FSC's defined for ASM are also forbidden here, and a recurrent configuration must burn completely. However, the SMAI steady state allows many more configurations than in ASM, for example, with heights 4 or above. These states do not occur with equal weights.

To use the rotational symmetry of the system the sandpile is grown with  $h_c=3$  within a circular region of radius  $R=(L-1)/2$  placed on a square lattice of size  $L \times L$ . In the steady state starting from the boundary the average height grows quickly radially towards the center following a power law:  $\langle h(r) \rangle = A - B(R-r)^{-\delta}$ , where  $r$  is the radial distance measured from the center. We estimate  $A=2.3904$ ,  $B=7.81$ , and  $\delta=0.75$  for  $L=1025$  (Fig. 2). The average height per site is found to depend on  $L$ , which on plotting with  $1/L$  extrapolates to a value 2.3840 in the limit of  $L \rightarrow \infty$ . Similar analysis yields the fraction of sites with different column heights are approximately  $2.1 \times 10^{-4}$  ( $h=0$ ), 0.2421 ( $h=1$ ), 0.3059 ( $h=2$ ), 0.3404 ( $h=3$ ). Beyond  $h=3$ , this fraction decreases approximately exponentially as  $\exp(-\alpha h)$ , where  $\alpha=1.64$  and adds up to a total of 0.1118.

The size of the avalanche is measured in three different

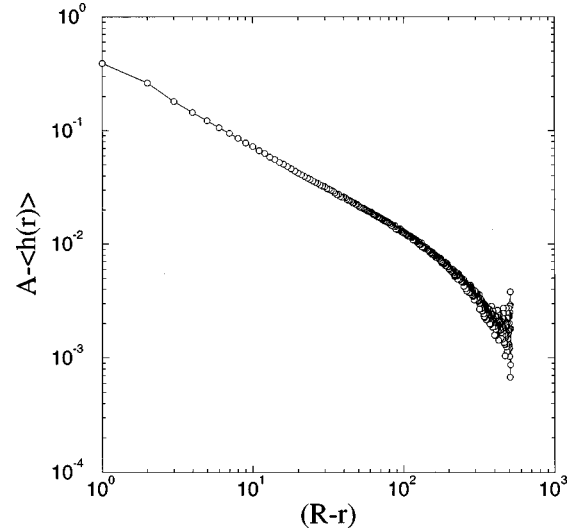


FIG. 2. The average height profile of the sandpile in a circular region plotted with the distance from the circumference of the circle is shown. The slope of the curve is 0.75 and  $A=2.3904$  is found.

ways: (i) the total number sites  $s$  that cross the threshold  $h_c$  (either toppled or not, both counted) (ii) the lifetime of the avalanche ( $t$ ), and (iii) the linear extent or the radius ( $r$ ) of the avalanche. Since  $s$ ,  $t$ , and  $r$  are the three different measurements of the same random avalanche cluster, they are necessarily dependent variables. These quantities are assumed to depend on one another as  $s \sim t^{\gamma_{ts}}$ ,  $r \sim t^{\gamma_{tr}}$ , and  $s \sim r^{\gamma_{rs}}$  and are connected by the relation  $\gamma_{ts} = \gamma_{tr} \gamma_{rs}$ .

To estimate the exponents  $\gamma_{ts}$  and  $\gamma_{tr}$  we measure the avalanche size  $s$  and avalanche radius  $r$  at every time step  $t$  during the progress of each avalanche. The total number of topplings up to time  $t$  gives the intermediate size  $s$  where as the size of the smallest square that encloses the cluster gives the intermediate radius  $r$ . We estimate  $\gamma_{ts}=1.64$  and  $\gamma_{tr}=0.83$ . Since the avalanche clusters are quite compact and have only few small holes it is justified to assume that  $\gamma_{rs}=2$ . These values are consistent to one another.

We assume the finite size scaling forms for the probability distribution functions as

$$P(s) \sim s^{-\tau_s} f_s\left(\frac{s}{L^{\sigma_s}}\right), \quad P(t) \sim t^{-\tau_t} f_t\left(\frac{t}{L^{\sigma_t}}\right),$$

$$P(r) \sim r^{-\tau_r} f_r\left(\frac{r}{L^{\sigma_r}}\right). \quad (1)$$

Consequently the cumulative probability distribution  $F(x) = \int_x^{L^{\sigma_x}} P(x) dx$  varies as  $x^{1-\tau_x}$ . However, in the case of  $\tau_x=1$ , the variation should be in the form  $F(x) = C - \ln(x)$ .

We plot the data of  $F(s)$  in two different ways. In Fig. 3 we plot  $F(s)$  vs  $s$  for system sizes  $L=65, 257$  and  $1025$  using a log-lin scale. Presence of humps in the large  $s$  limit is visible for bigger system sizes, which reflects the effect of the finite system size on power-law distributions. However, in the intermediate region curves are reasonably straight, indicating that the exponent  $\tau_s$  is likely to be 1. We further plot  $F(s)s^{\tau_s(L)-1}$  with  $s$  on a log-log scale and tune  $\tau_s(L)$ , the effective  $\tau_s$  exponent for the system size  $L$ , such that the

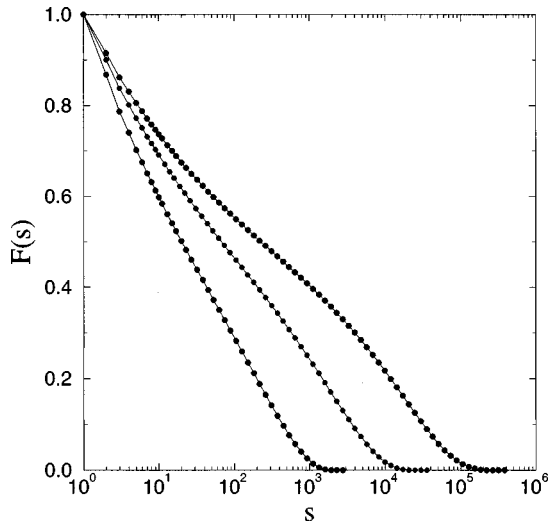


FIG. 3. Log-lin plot of the cumulative probability distribution  $F(s)$  for the three system sizes  $L=65, 257,$  and  $1025$  (from left to right). The straight portions of the curves in the intermediate regions indicates that  $\tau_s$  is likely to be equal to 1.

curves become horizontal in the intermediate range of  $s$ . All three curves collapse nicely when the abscissa is scaled as  $sL^{-1.62}$ , which implies that  $\sigma_s = 1.62$ . We show in the Fig. 4 that the  $\tau_s(L)$  values very closely fit to a straight line when plotted with  $L^{-1/4}$ . It seems that  $L^{-1/4}$  may be the right leading correction to scaling. The fitted straight line when extrapolated to  $L \rightarrow \infty$  gives a value of 1.016 for  $\tau_s$ . Similar analysis for the lifetime distribution also leads us to conclude that  $\tau_t = 1.02, \sigma_t = 0.98$ . The radius distribution  $F(r)$  is calculated in a different way: the probability that a site at a distance  $r$  from the center of mass of the avalanche cluster belongs to the cluster. In Fig. 5 we show a scaling plot  $F(r)L^{0.20}$  against  $rL^{-0.86}$  using a log-lin scale for different system sizes. Here we see a much better straight part in the intermediate region. We conclude a value of  $\tau_r \approx 1$ .

The distribution functions follow relations like  $P(s)ds \sim P(t)dt$  that imply following scaling relations,

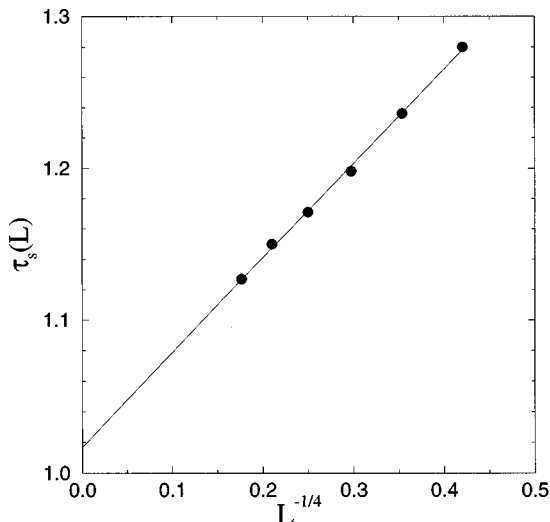


FIG. 4. Plot of  $\tau_s(L)$  for different system sizes  $L=33, 65, 129, 257, 513,$  and  $1025$  with  $L^{-1/4}$ . A direct straight line fit gives  $\tau_s = 1.016$  in the  $L \rightarrow \infty$  limit.

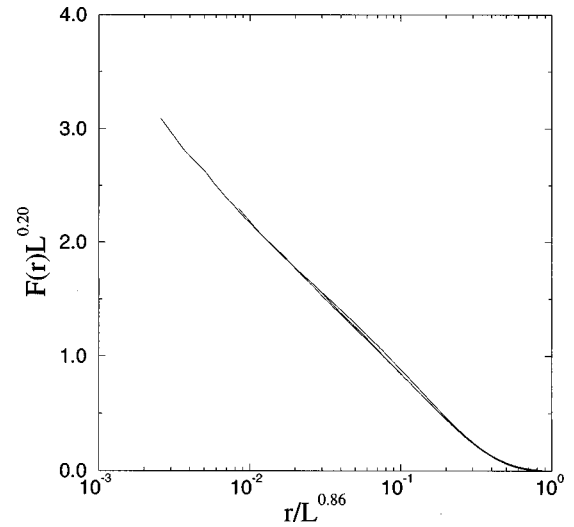


FIG. 5. Scaling plot of the cumulative radial distribution function  $F(r)$ . Plot of  $F(r)L^{0.20}$  vs  $r/L^{0.86}$  shows the data collapse for the system sizes  $L=65, 257,$  and  $1025$ .

$$\begin{aligned} \tau_s - 1 &= \gamma_{ts}(\tau_t - 1), & \tau_r - 1 &= \gamma_{tr}(\tau_t - 1), \\ \tau_s - 1 &= \gamma_{rs}(\tau_r - 1). \end{aligned} \quad (2)$$

These equations imply that if one of the exponents  $\tau_s, \tau_t$  or  $\tau_r$  is equal to 1, the rest are also equal to 1, irrespective of the values of the  $\gamma$  exponents. Our estimates for the different  $\tau$  exponents are very much consistent with these equations. We also observe that the value of  $\tau_s \approx 1$  agrees very well with Zhang's result  $\tau_s = 2(1 - 1/d)$  for  $d = 2$  [16].

We also assume that the average values of  $s, t,$  and  $r$  vary with the system size  $L$  as  $\langle s(L) \rangle \sim L^{\beta_s}, \langle t(L) \rangle \sim L^{\beta_t},$  and  $\langle r(L) \rangle \sim L^{\beta_r}$ . We plot  $\langle s(L) \rangle$  vs  $L$  on a log-log scale for  $L = 33, 65, 129, 257, 513,$  and  $1025$ . Slopes between successive points are plotted with  $L^{-2}$  and extrapolated to the  $L \rightarrow \infty$  limit giving  $\beta_s = 1.61$ . Similar analysis gives  $\beta_t = 0.96$  and  $\beta_r = 0.82$ .

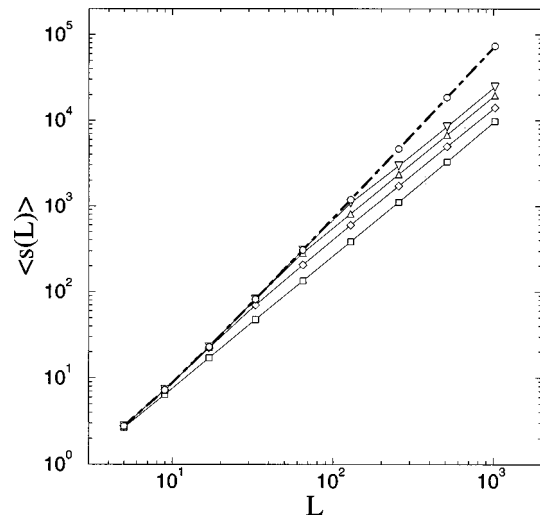


FIG. 6. Plot of  $\langle s(L) \rangle$  versus  $L$  for  $m = 1, 2, 4,$  and  $8$  of SMAI (solid lines) and for ASM (dot dashed line). For each value of  $m$  there is a threshold system size  $L$  at which the crossover from ASM behavior to SMAI takes place.

Using the scaling forms in Eq. (1) we get following scaling relations for  $\beta$  exponents as  $\beta_s = \sigma_s(2 - \tau_s)$ ,  $\beta_t = \sigma_t(2 - \tau_t)$ , and  $\beta_r = \sigma_r(2 - \tau_r)$ . With our measured values of  $\beta$ ,  $\sigma$ , and  $\tau$  these relations are approximately satisfied. We set errors of 0.05 to all our measured exponents.

Next we study the case when there is a cutoff for the toppling number  $m > 1$ . The average cluster size  $\langle s(L) \rangle$  is plotted with  $L$  on the log-log scale in Fig. 6 for  $m = 1, 2, 4$ , and 8. We see that all curves are parallel straight lines with slopes approximately 1.61 for large system sizes. However, for small system sizes all of them bend and become part of the same straight line. Then we plot on the same figure the  $\langle s(L) \rangle$  data for ASM. We get a straight line with a slope  $\approx 2$  that almost overlaps with the bend portions of the curves for different  $m$  values. We explain this by noting that for every  $m$  value our model behaves as the ASM for small system sizes. In small systems the number of avalanches where sites will topple more than  $m$  times are very few.

However for bigger system sizes the cutoff  $m$  will have more prominent effects. Therefore, for each  $m$  value there should be one particular system size where the crossover takes place from ASM to non-Abelian behavior. The crossover size  $L_c \sim m$  is observed. We expect that for any  $m$  value if one works in systems larger than the crossover size one should get the same set of exponents as those in the case of  $m = 1$ .

To summarize, we studied here a new sandpile model where bonds of the system relax after a certain number of transmission of grains. This limits a site to topple a maximum of  $m$  times within the same avalanche. Based on the results of detailed numerical studies using improved algorithms we claim a crossover from ASM behavior to a new critical behavior at a particular size of the system whose magnitude depends on the value of  $m$ .

We acknowledge with thanks D. Dhar and V. B. Priezzhev for many useful discussions and suggestions. D. G. gratefully acknowledges financial support from the Indo-French Centre for the Promotion of Advanced Research (IF-CPAR).

- 
- [1] P. Bak, C. Tang, and K. Wiesenfeld, Phys. Rev. Lett. **59**, 381 (1987); Phys. Rev. A **38**, 364 (1988); P. Bak, *How Nature Works: The Science of Self-Organized Criticality* (Copernicus, New York, 1996).
- [2] G. A. Held, D. H. Solina II, D. T. Keane, W. J. Haag, P. M. Horn, and G. Grinstein, Phys. Rev. Lett. **65**, 1120 (1990); V. Frette, K. Christensen, A. Malte-Sorensen, J. Feder, T. Josang, and P. Meakin, Nature (London) **379**, 49 (1996).
- [3] P. Bak and K. Chen, Physica D **38**, 5 (1989).
- [4] H. Takayasu and H. Inaoka, Phys. Rev. Lett. **68**, 966 (1992); A. Rinaldo, I. Rodriguez-Iturbe, R. Rigon, E. Ijjasz-Vasquez, and R. L. Bras, *ibid.* **70**, 822 (1993); S. S. Manna and B. Subramanian, *ibid.* **76**, 3460 (1996).
- [5] J. M. Carlson and J. S. Langer, Phys. Rev. Lett. **62**, 2632 (1989); A. Sornette and D. Sornette, Europhys. Lett. **9**, 197 (1989); Z. Olami, H. J. S. Feder, and K. Christensen, Phys. Rev. Lett. **68**, 1244 (1992).
- [6] L. P. Kadanoff, S. R. Nagel, L. Wu, and S. Zhou, Phys. Rev. A **39**, 6524 (1989); S. S. Manna, Physica A **179**, 249 (1991).
- [7] D. Dhar, Phys. Rev. Lett. **64**, 1613 (1990); S. N. Majumdar and D. Dhar *ibid.* **185**, 129 (1992); E. V. Ivashkevich, D. V. Kvitarev, and V. B. Priezzhev, Physica A **209**, 347 (1994).
- [8] S. S. Manna, J. Stat. Phys. **59**, 509 (1990); P. Grassberger and S. S. Manna, J. Phys. (France) **51**, 1077 (1990).
- [9] V. B. Priezzhev, D. V. Kvitarev, and E. V. Ivashkevitch, Phys. Rev. Lett. **76**, 2093 (1996).
- [10] M. Paczuski and S. Boettcher, Phys. Rev. E **56**, 3745 (1997).
- [11] S. S. Manna, J. Phys. A **24**, L363 (1992).
- [12] A. Vespignani, S. Zapperi, and L. Pietronero, Phys. Rev. Lett. **72**, 1690 (1994); Phys. Rev. E **51**, 1711 (1995).
- [13] A. Ben-Hur and O. Biham, Phys. Rev. E **53**, R1317 (1996); H. Nakanishi and K. Sneppen, *ibid.* **55**, 4012 (1997).
- [14] B. Tadic and D. Dhar, Phys. Rev. Lett. **79**, 1519 (1997).
- [15] D. Dhar, Physica A **186**, 82 (1992).
- [16] Y-C. Zhang, Phys. Rev. Lett. **63**, 470 (1989).